

AD-A283 171



Public reporting burden  
gathering and mainte-  
nance of information  
this form, including the  
time for reviewing instructions, searching existing data sources,  
information. Send comments regarding this burden estimate or any other aspect of this  
dquarters Services, Directorate for Information Operations and Reports, 1215 Jefferson  
Budget, Paperwork Reduction Project (0704-0188), Washington, DC 20503.

AGE

Form Approved  
OMB No. 0704-0188

1. AGENCY USE ONLY (Leave blank)

2. REPORT DATE

3. REPORT TYPE AND DATES COVERED

4. TITLE AND SUBTITLE

SPATIAL INFORMATION CONTENT ANALYSIS OF  
WIENER SPECTRA FROM POLARIZED WATER  
WAVE IMAGERY

5. FUNDING NUMBERS

6. AUTHOR(S)

JAN A. NORTH, Capt, USAF

7. PERFORMING ORGANIZATION NAME(S) AND ADDRESS(ES)

SYRACUSE NEW YORK

8. PERFORMING ORGANIZATION  
REPORT NUMBER

44101

9. SPONSORING/MONITORING AGENCY NAME(S) AND ADDRESS(ES)

DEPARTMENT OF THE AIR FORCE  
AFIT/CI  
2950 P STREET  
WRIGHT-PATTERSON AFB OH 45433-7765

10. SPONSORING/MONITORING  
AGENCY REPORT NUMBER

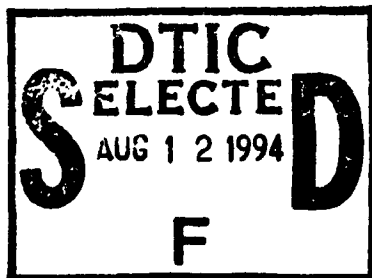
11. SUPPLEMENTARY NOTES

12a. DISTRIBUTION/AVAILABILITY STATEMENT

Approved for Public Release IAW 190-1  
Distribution Unlimited  
MICHEAL M. BRICKER, SMSgt, USAF  
Chief Administration

12b. DISTRIBUTION CODE

13. ABSTRACT (Maximum 200 words)



14. SUBJECT TERMS

15. NUMBER OF PAGES

33

16. PRICE CODE

17. SECURITY CLASSIFICATION  
OF REPORT18. SECURITY CLASSIFICATION  
OF THIS PAGE19. SECURITY CLASSIFICATION  
OF ABSTRACT

20. LIMITATION OF ABSTRACT

## GENERAL INSTRUCTIONS FOR COMPLETING SF 298

The Report Documentation Page (RDP) is used in announcing and cataloging reports. It is important that this information be consistent with the rest of the report, particularly the cover and title page. Instructions for filling in each block of the form follow. It is important to *stay within the lines* to meet optical scanning requirements.

### Block 1. Agency Use Only (Leave blank).

**Block 2. Report Date.** Full publication date including day, month, and year, if available (e.g. 1 Jan 88). Must cite at least the year.

**Block 3. Type of Report and Dates Covered.** State whether report is interim, final, etc. If applicable, enter inclusive report dates (e.g. 10 Jun 87 - 30 Jun 88).

**Block 4. Title and Subtitle.** A title is taken from the part of the report that provides the most meaningful and complete information. When a report is prepared in more than one volume, repeat the primary title, add volume number, and include subtitle for the specific volume. On classified documents enter the title classification in parentheses.

**Block 5. Funding Numbers.** To include contract and grant numbers; may include program element number(s), project number(s), task number(s), and work unit number(s). Use the following labels:

C - Contract	PR - Project
G - Grant	TA - Task
PE - Program Element	WU - Work Unit Accession No.

**Block 6. Author(s).** Name(s) of person(s) responsible for writing the report, performing the research, or credited with the content of the report. If editor or compiler, this should follow the name(s).

**Block 7. Performing Organization Name(s) and Address(es).** Self-explanatory.

**Block 8. Performing Organization Report Number.** Enter the unique alphanumeric report number(s) assigned by the organization performing the report.

**Block 9. Sponsoring/Monitoring Agency Name(s) and Address(es).** Self-explanatory.

**Block 10. Sponsoring/Monitoring Agency Report Number.** (If known)

**Block 11. Supplementary Notes.** Enter information not included elsewhere such as: Prepared in cooperation with...; Trans. of...; To be published in.... When a report is revised, include a statement whether the new report supersedes or supplements the older report.

**Block 12a. Distribution/Availability Statement.** Denotes public availability or limitations. Cite any availability to the public. Enter additional limitations or special markings in all capitals (e.g. NOFORN, REL, ITAR).

DOD - See DoDD 5230.24, "Distribution Statements on Technical Documents."

DOE - See authorities.

NASA - See Handbook NHB 2200.2.

NTIS - Leave blank.

### Block 12b. Distribution Code.

DOD - Leave blank.

DOE - Enter DOE distribution categories from the Standard Distribution for Unclassified Scientific and Technical Reports.

NASA - Leave blank.

NTIS - Leave blank.

**Block 13. Abstract.** Include a brief (Maximum 200 words) factual summary of the most significant information contained in the report.

**Block 14. Subject Terms.** Keywords or phrases identifying major subjects in the report.

**Block 15. Number of Pages.** Enter the total number of pages.

**Block 16. Price Code.** Enter appropriate price code (NTIS only).

**Blocks 17 - 19. Security Classifications.** Self-explanatory. Enter U.S. Security Classification in accordance with U.S. Security Regulations (i.e., UNCLASSIFIED). If form contains classified information, stamp classification on the top and bottom of the page.

**Block 20. Limitation of Abstract.** This block must be completed to assign a limitation to the abstract. Enter either UL (unlimited) or SAR (same as report). An entry in this block is necessary if the abstract is to be limited. If blank, the abstract is assumed to be unlimited.

94 101

**SPATIAL INFORMATION CONTENT  
ANALYSIS OF WIENER SPECTRA FROM  
POLARIZED WATERWAVE IMAGERY**

BY

Jan A. North, Capt, USAF  
(AFIT / CIRD)

A proposal for Ph.D. thesis research  
to be performed at the  
State University of New York  
College of Environmental Science & Forestry  
Syracuse New York

15 March 1994

Dr. Michael Duggin, Thesis Advisor

Accession For	
NTIS CRA&I	<input checked="" type="checkbox"/>
DTIC TAB	<input type="checkbox"/>
Unannounced	<input type="checkbox"/>
Justification	
By	
Distribution /	
Availability Codes	
Dist	Avail and/or Special
A-1	

35P8 94-25396



1

94 8 11 106

## **ABSTRACT**

This study proposes to analyze the correlation sensitivity of spatial Wiener spectra derived from polarized (Stokes' parameter) imagery of both synthetic and measured waterwave scenes. The intent of this study is to evaluate the utility of polarized imagery in the extraction of spatial information content (to include texture) from scenes containing waterwaves, one of many spatially correlated natural features that can be described by Wiener spectra.

This study will first enhance an existing simulation model [North, 1989] to support the comparison of the spatial performance of an imaging system through the creation of synthetic polarized images of waterwave scenes and their spatial spectra. Second, this model will be tailored to a specific imaging system: differentially polarized 4-lens 35-mm photography. Third, a parametric exploration of the model will be used to predict the polarized imaging conditions that optimize spatial information content. Fourth, a polarized 4-lens camera system will collect representative imagery containing waterwave scenes under natural conditions. Finally, the synthetic and measured polarized image spectra will be analyzed and compared in order to validate the simulation model, calibrate the imaging system, and ultimately provide the basis for the utility evaluation.

The results of this study should provide a refined understanding of the contribution that sensed polarization can provide in the analysis of spatial information content from imagery, through the detailed examination of its effect on natural waterwave surfaces.

## **1.0 PURPOSE**

The purpose of this study is to evaluate the utility of polarized (Stokes' parameter) imagery in the extraction of spatial information content from scenes of waterwaves, one of many spatially correlated natural features that can be described by Wiener spectra. The primary method of evaluation is correlation sensitivity analysis of the synoptic spatial spectra derived from the polarized imagery.

This investigation will be executed in three parts:

1) synthesize a reasonable model which can consider the effects of resolving differentially polarized spatial image spectra of waterwave scenes under various illumination, scene, and sensor geometries; tailor the model for a specific imaging system - differentially polarized 4-lens 35-mm photography; and exercise the model to define the parametric dependencies for correlation between the actual (modeled) waterwave slope spectra and their reconstructions from the polarized radiance distributions captured by imagery,

2) execute a controlled experiment: photograph representative waterwave surfaces under natural illumination conditions by a differentially polarized 4-lens 35-mm camera system, using the model predictions to specify the range of imaging conditions that

should enhance the correlation sensitivity analysis, and

3) analyze and compare both the synthetic and measured polarized image spectra; attempt to validate the simulation model; attempt to calibrate the imaging system; and provide a utility evaluation.

The prime motivation for this study is to extend an existing simulation model of one spatially correlated natural feature (waterwaves) as a basis for the study of other natural background and clutter features (definable by Wiener spectra) under polarized imaging conditions. However, this simulation model is unvalidated, hence a second motivation is to calibrate the model through the analysis of, and comparison with, actual polarized image data. A third motivation is to consider the potential utility of polarized waterwave scenes as natural opportunistic targets for synoptic image calibration. This motivation is based on several unique aspects of water and waterwaves that are enumerated below. A fourth, and final, motivation is to demonstrate the feasibility of extending this analysis to more complex imaging systems, e.g., synthetic aperture radar (SAR) polarimetry, using simpler optical techniques for this study.

There are several reasons for selecting natural waterwave surfaces as the object of polarized image spectrum analysis:

1) Terrestrial surface water is ubiquitous; fully three

quarters of the Earth's surface is covered with water. For airborne and spaceborne sensors, this represents a large window of opportunity to image this target.

2) In comparison with other terrestrial surface features, water surfaces are optically homogeneous; only two radiance functions, one for surface reflection and one for upwelling subsurface refraction, are required to describe the unique radiance contribution of the imaged water scene. However, in the red (and at longer wavelengths), water is increasingly opaque to the point that only surface reflection (and/or emission in the infrared) requires description.

3) Except for the rare instances of sustained windlessness where water is smooth and specular, its surface is disturbed by the addition of directional friction energy applied by wind passing over it. Up to a defined maximum wind velocity, the disturbed surface remains analytic (infinitely differentiable) and can be described as a quasi-stationary, pseudo-Gaussian process; the resulting power spectrum approximations for elevation, slope, and curvature can be analyzed by Fourier methods [Kinsman, 1965].

4) As an extension of 3) above, waterwaves can be imaged over several orders of spatial frequency. Also, the well-behaved surface statistics of waterwave surfaces (e.g., mean slope =  $0^\circ$ , 3-sigma slope  $\ll 30^\circ$ ) allow for a broad range of off-vertical imaging

geometries without having to consider the complex effects of surface obscuration.

5) Also as an extension of 3), the assumption of quasi-spatial and quasi-temporal invariance of the surface spectra allows for considerable tolerance in both image collection and processing: precise pointing to an exact ground reference point by multiple sensors is not critical; precise collection timing by multiple sensors is not critical; and image registration is not required.

6) Finally, the natural air-water interface represents a strong polarizing dielectric. High contrasts within and between polarized images should be readily detectable in a significant range around mean-Brewster-angle imaging geometries.

In sum, this study will exploit one of the more analytically straightforward terrestrial surface features for the evaluation of polarized (Stokes' parameter) imagery in the extraction of texture information from scenes of spatially correlated natural features that can be described by Wiener spectra.



## **2.0 LITERATURE REVIEW**

### **2.1 Image Analysis of Waterwave Surfaces**

In 1925, Schumacher made near-horizontal stereo-pairs from a ship with the intent of measuring the variability of wave heights. The utility of this method was severely limited due to many factors: 1) the camera baseline was restricted to the length of the ship; 2) waves in the foreground obstructed waves in the background; 3) backsides of waves were not visible; and 4) there was a lack of 'ground' control on the open seas for height determination - the errors are especially pronounced from an oblique perspective [Pos,1988]. This experiment represents a limiting case for waterwave surface measurement via image analysis.

In 1933, Hulburt [1934] made polarized and unpolarized oblique photographs of sun glitter on sea waves to measure the polarization of light at sea with respect to surface roughness, sun angle, and weather conditions. Because the widths of glitter patterns correlate to the maximum slope of the sea surface, Hulburt was able to demonstrate that waves in the North Atlantic varied from 15° inclination when winds were blowing at 3 knots up to 25° inclination at 18 knots.

Sawyer [1949] mounted a Sonne strip camera on a fast low-flying airplane to photograph narrow strips of the sea surface and

measure the directional spectrum of the waves. The field of view was too narrow to capture significant amounts of surface data orthogonal to the flightline. The accuracy of the spectral estimate decreased with the angle from the flightline.

Also in 1949, Barber [1949,1954] analyzed single photographs of sea surfaces to determine wave direction, but he was unable to determine the two-dimensional spectrum due to the computing limitations of the time. At this point, it became apparent that an essential requirement for future analysis of waterwave surfaces was to have near-nadir, high resolution, high-contrast images covering large areas. The intent was to photographically capture significant information about the largest range of spatial frequency components without perspective distortion or hidden surface detail. It also became apparent that the analysis of large amounts of spatial information required the power of a digital computer.

In 1951, Cox and Munk [1954a,b] measured the wave-slope distributions of the sea surface from aerial photographs of sun glitter patterns. They computed the distribution from the measured variation of radiance within a glitter pattern instead of computing maxima from the pattern boundaries as done by Hulburt. Four cameras were flown from a single airplane at altitudes of 2000 feet, with two used as imagers and two used as radiometers. Their image analysis was quite sophisticated; it accounted for sun diameter, angular reflectivity, lens falloff (vignetting), film sensitivity,

exposure calibration (sensitometry), and ultimately provided a first-order relationship between film density and directional wave-slope probability.

In 1953, Schooley [1954] performed a simplified version of the Cox & Munk experiment by taking flash photographs of a river surface from a 45-foot bridge elevation at night. The main limitation of his experiment was the probable inhomogeneity of the water surface due to limited fetch and the presence of wave-refracting obstacles in the water.

In 1954, medium-altitude (3000 feet) stereophotography was employed by Marks and Ronne [1955] to generate stereopairs of sea surfaces. Two airplanes carried radio-synchronized cameras and a surface ship acted as 'ground' control in the photographs. Elevations were photogrammetrically measured at discrete points and the sampled elevation array was then autocorrelated (the sampling distance determined the desired spatial resolution). This experiment marks the first recorded use of a digital computer to calculate the directional 2D spectra of waterwaves. The work of Cote et al. [1960] enhanced this basic technique. More recent stereophotogrammetric efforts include Holthuijsen [1983a,b] and Pos et al. [1988]. Elements of this later work include methods to render the water opaque so that a more exact calculation of the height field can be made.

During the 1950s and early 1960s, Longuet-Higgins [1952-1962; Cartwright & Longuet-Higgins, 1956] elaborated on the results of Cox and Munk to formulate the statistical theory of patterns, paths, number, frequency, and distributions of specular reflection points on randomly moving surfaces. Stilwell [1969; Stilwell & Pilon, 1974] correlated the statistics of sea-surface images to the wave-slope statistics of the actual sea surface. Under the assumptions of uniform sky radiance, optimized viewing geometry, and small surface slopes, Stilwell derived the relationship between the film transmittance of an imaged surface point and the range component of the wave slope at that surface point. He further demonstrated a linearizable relationship between the spatial image spectrum and the imaged surface slope spectrum. Kasevitch [1975] extended Stilwell's model to second order to develop an optimization criterion for the relationship. Chapman and Irani [1981] took this work one step further by creating a synthetic model and executing a limited quantification of the error magnitudes associated with the parametric dependence of this linear model.

Sheres [1980] developed a novel technique for remotely sensing surface-flow velocities based on imagery of monochromatic wavetrains of known frequency (such as those generated by a motor boat) propagating over the region of interest. His work demonstrated that the wavelength and direction of two different wavetrains produced all the information required to calculate surface flows. Gotwols and Irani [1980] developed a similar

technique to determine the phase velocity of short gravity waves.

Exotic sensors using LASER [Palm et al.,1977; Schau,1978; Abshire & McGarry,1987] and LIDAR [Weinman,1988] have been used to extract directional spectra and surface backscatter data at higher wavenumbers (i.e., the capillary wave regime). Synthetic Aperture Radar (SAR) imagery has been used to estimate spectra, phase velocities, and propagation directions at lower wavenumbers (i.e., the gravity wave regime) [Monaldo & Lyzenga,1986; Monaldo & Kasevich,1982; Carlson,1984]. Also, Long Wave Infrared (LWIR) sensors have been used to calculate spatial spectra of ocean-surface temperature [Saunders,1967,1968; McLeish,1970].

Lybanon [1985] reported on the implementation of an automated image-analysis system by the U.S. Naval Ocean Research & Development Activity (NORDA). The Interactive Digital Satellite Image Processing System (IDSIPS) can automatically derive the sea-surface slope statistics from sun glitter images through analysis of the imaging geometry. As a late practical example, Fisher [1986] analyzed four sun glitter images taken from the space shuttle Challenger (STS-41G) to locate acoustically important oceanographic features in support of hydro-acoustical sensor placement.

## 2.2 Spatial Spectrum Analysis of Waterwave Scenes

A comprehensive review would include the work of Stillwell and Pilon [1974], and Kasevich et al. [1971,1972]. The emphasis of this earlier work is on the analysis of coherent optical processing techniques as applied to photographic emulsions of wave scenes. Kasevich [1975] provides a general introduction to the first-order theory subsequent to the development of an geometric-optics-approximation second-order theory that estimates the optimum viewing geometry for obtaining reasonable spectra. Stillwell [1969] provides additional development of optical imaging theory subsequent to performing an optical analysis to derive directional wave spectra. Only the first-order theory is reviewed here; Kasevich's second-order theory is outside the scope of this study since it assumes simplified approximations for both Fresnel reflectivity and sky radiance distributions. However, the most general results of a second-order theory can be compared, with caution, to the results of this study; any second-order theory loses definiteness because the spatial distributions for natural radiance are independent, i.e., no general solution can be specified [Stillwell,1969]. This is the prime motivation for the synthesis and analysis of geometric effects through the use of analytic models.

## Review of Kasevich [1975]

The essential requirement for the determination of spectra from wave images is to have the spatial modulation of the image be proportional to the wave profile. Kasevich uses the example of a transparency with film exposure,  $E$ , defined over its linear region by

$$E(y) = [f_0(y)]^{-\frac{\gamma}{2}} \times \left[ \frac{1+f(y)}{f_0(y)} \right]^{-\gamma/2} \quad [2.2:1]$$

where

$$E(y) = f_0(y) + f(y), \quad [2.2:2]$$

such that

$f_0(y)$  - the mean exposure on film,

$f(y)$  - the exposure modulation due to scattering of radiance from specular wave-slope facets, and

$\gamma$  - the film gamma. This example is given for a two-dimensional case.

If  $f_0(y) \gg f(y)$ , then Equation [2.2:1] can be expanded in a binomial series to yield the approximation

$$E(y) \approx [f_0(y)]^{-\frac{\gamma}{2}} \times \left[ 1 - \frac{\gamma}{2} \frac{f(y)}{f_0(y)} \right] \quad [2.2:3]$$

The estimation of the slope spectrum from the forward Fourier transform of the image requires that  $f(y)$  be linear with respect to the wave slope  $dz/dy$ , where  $z$  is the surface elevation. This condition can only be approximately satisfied because of the nonlinearity of 1) the spatial radiance distributions found in nature, 2) the Fresnel reflectivity variation with respect to incidence angle, and 3) the refraction of upwelling subsurface radiance in the direction of the observer.

#### Review of Stillwell [1969]

For a small wave-slope angle  $\beta$ , the small angle approximation is:

$$\beta = \tan^{-1}\left(\frac{dz}{dy}\right) \approx \frac{dz}{dy} \quad [2.2:4]$$

where  $\beta$  is the fundamental parameter for extracting wave-slope spectra from imagery. The law of Malus defines the radiance observed at azimuth angle  $\theta$  as a simple function of Fresnel reflectivity and incident radiance:

$$L_0(\theta, \beta, \omega) = L(\mu) \times R(\omega) \quad [2.2:5]$$

where

$$L_0(\theta, \beta, \omega) = \text{the observed reflected radiance,}$$



$L(\mu)$  - the incident radiance to be reflected,  
 $R(\omega)$  - the Fresnel reflectivity (for any arbitrary polarization),  
 $\theta$  - the zenith angle of observation,  
 $\beta$  - the slope of the reflecting surface facet,  
 $\mu$  - the zenith angle of the incident radiance, and  
 $\omega$  - the angle of incidence, such that

$$\omega = \theta - \beta \quad [2.2:6]$$

and

$$\mu = \omega - \beta \quad [2.2:7]$$

Figure 2.2:1 illustrates the angular relations in two dimensions.

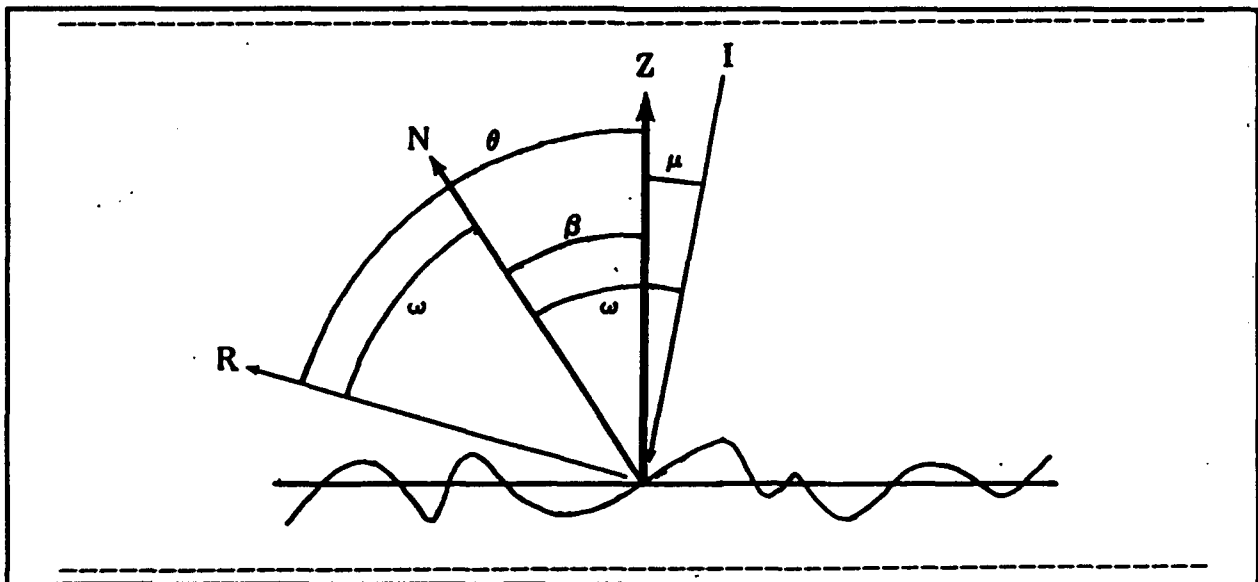


FIGURE 2.2:1. Angular Relations for the 2-D case.

The variation of observed radiance with respect to a change of surface slope  $d\beta$  at some point is

$$\frac{dL(\theta)}{d\beta} = \frac{dL(\mu)}{d\mu} \frac{d\mu}{d\beta} + L(\mu) \frac{dR(\omega)}{d\omega} \frac{d\omega}{d\beta} \quad [2.2:8]$$

If  $\beta$  is a small angle and

$$\omega \approx \mu, \quad [2.2:9]$$

then

$$\frac{dL(\theta)}{d\beta} = [L'(\mu) * R(\omega) + L(\mu) * R'(\omega)] * \frac{d\omega}{d\beta}, \quad [2.2:10]$$

where the prime (') denotes the first derivative with respect to the argument. With the assumption that the water surface remains analytic, the small-angle linear approximation holds in the Fourier transform for wave-slope angles ( $\beta$ ) up to at least  $30^\circ$  [Stillwell, 1969].

#### Review of Chapman and Irani [1981]

The intent of Chapman and Irani was to quantify the parametric dependencies of errors inherent in linearly relating a wave-slope magnitude spectrum to the corresponding radiance image magnitude spectrum. Their approach was to simulate radiance images of wind-driven water-wave surfaces in three dimensions. Their simulation utilized empirical models of the water surface, the sky radiance

surface slope to radiance. They determined that the three-dimensional simulation was computationally expensive so only a small number of geometries were investigated. However, they initially used a simpler two-dimensional model of a  $\pm 15^\circ$  sinusoidal wave propagating in a single direction along the sensor field in order to survey various geometries for further synthesis and analysis in three dimensions.

Figure 2.2:2 illustrates the three-dimensional methodology for image synthesis and error analysis used by Chapman and Irani.

Chapman and Irani then applied their three-dimensional model to six selected geometries. Their results indicated 1) nonlinearities are largely independent of wavenumber, 2) nonlinearities remain relatively low (error < 3 dB) over a relatively wide range of azimuth ( $100-120^\circ$ ) around the sensor azimuth, and 3) nonlinearities increase within  $30-40^\circ$  of the cross-field direction.

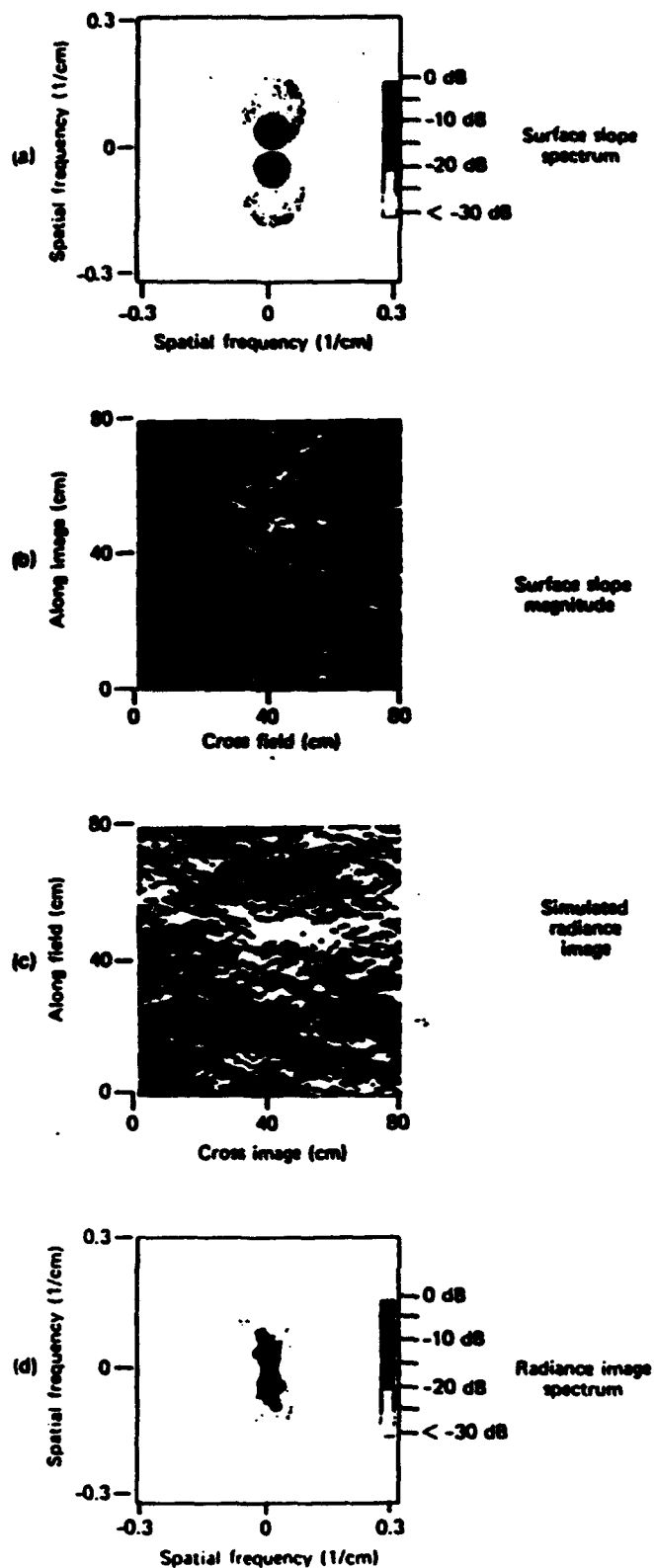


FIGURE 2.2:2. 3-D methodology of Chapman & Irani [1981].

## **Review of North [1989]**

North amplified and extended the work of Chapman and Irani [1981] based on a proposed statement of work:

"An exhaustive evaluation of our radiance modulation model would involve: 1) simulating the geometry of a surface area; 2) transforming that surface geometry into an image using a particular set of optical conditions; 3) estimating the slope spectrum of the simulated surface and the spectrum of the image; 4) repeating steps 1-3 for all other possible imaging geometries; and 5) comparing each image spectrum with the corresponding slope spectrum to obtain estimates of the error arising from nonlinearity. This, in fact, is impractical because there are a large number of parameters to be varied, and, for any set of these parameters, the error computations involves a large number of operations." [Chapman & Irani, 1981]

The intent of this study was to develop and execute a test design which would provide a minimal yet sufficient set of parameters to both verify the limited results of Chapman & Irani and complete a more detailed parametric surface exploration. The more robust test design of this study recognized that what was computation-ally impractical in 1981 was quite doable with 1989 resources.

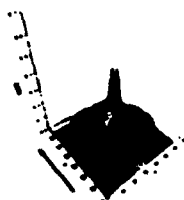
Figure 2.2:3 illustrates the three-dimensional methodology for image synthesis and error analysis used by North.

A nonlinear transformation of wave slope to reflected and refracted in both horizontal and vertical polarizations was effected under the special conditions of Brewster-angle viewing under clear skies at a wavelength of 460 nm. Seventy two syntheses

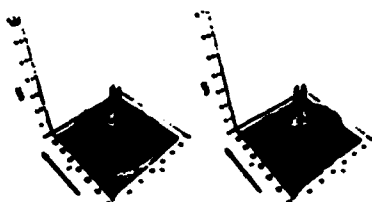
were varied with respect to six distinct solar positions, four distinct wind directions, and three distinct wind velocities.

The synthetic wave scenes were analyzed via the forward Fourier transformation and their radiance magnitude spectra were compared with the original slope magnitude spectra of the initial synthesis in order to estimate the effects of the nonlinear radiance transformation on the recovery of the wave slope spectrum from imagery. Within the boundaries of the study, the limited results of Chapman and Irani [1981] were more generally verified, the existence of an optimal imaging geometry for slope spectrum estimation was indicated, and sub-resolution wave slopes were found to produce a significant effect on the wave slope spectra derived from imagery.

SPECIFY SLOPE MAGNITUDE SPECTRUM  
(Equations 2.2:1-2.2:24)



RESOLVE INTO COMPONENT SPECTRA  
(Equations 2.2:25-2.2:26)



FILTER COMPONENT SPECTRA THROUGH  
WHITE NOISE & INVERSE FFT  
(Equations 2.2:27-2.2:29)

RESOLVE INTO SLOPE MAGNITUDE &  
SLOPE AZIMUTH ARRAYS  
(Equations 2.2:30-2.2:40)



SLOPE MAGNITUDE ARRAY (BETA)

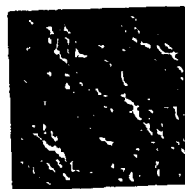
SLOPE AZIMUTH ARRAY (ALPHA)



TRANSFORM SLOPE-TO-RADIANCE

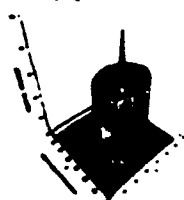


SYNTHETIC RADIANCE IMAGE



FORWARD FFT & GENERATE  
DIFFERENCE (ERROR) SPECTRA  
(Equations 2.8:1-2.8:11)

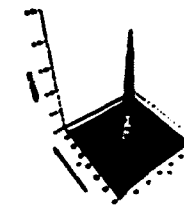
SYNTHESIZE SKYDOME DOWNWELLING  
RADIANCE (H & V POLARIZATION)  
(Equations 2.3:1-2.3:13)  
(Equations 2.5:17-2.5:29)



MULTIPLY BY SURFACE PROJECTION  
& FRESNEL REFLECTION COEFFICIENTS  
(Equations 2.5:1-2.5:9)  
(Equations 2.5:17-2.5:29)

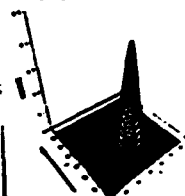
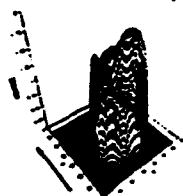


CORRELATE BY SUB-RESOLUTION  
WAVE SLOPE ATTENUATION FILTER  
(Equations 2.5:10-2.5:16)  
(Equations 2.5:17-2.5:29)

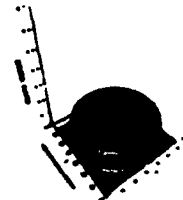


$L_r'(\text{BETA}, \text{ALPHA}) (\text{HORIZ})$

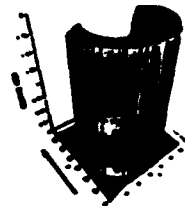
$L_r'(\text{BETA}, \text{ALPHA}) (\text{VERT})$



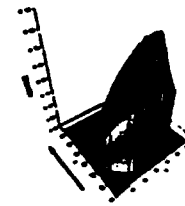
SYNTHESIZE SUBDOME UPWELLING  
RADIANCE (H & V POLARIZATION)  
(Equations 2.4:1-2.4:7)



MULTIPLY BY SURFACE PROJECTION  
COEFFICIENTS  
(Equation 2.6:1)



$L_u'(\text{BETA}, \text{ALPHA}) (\text{H} \& \text{V})$



TRANSFORM SLOPE-TO-RADIANCE



D2 SPECTRUM

D1 SPECTRA

FIGURE 2.2:3. 3-D methodology of North [1989].

### **3.0            APPROACH**

The proposed research project will have three phases: one phase is data synthesis (modeling & prediction); one phase is data collection (in-field photography & image processing); and one phase is data analysis (of the measured imagery & comparison with the synthetic model predictions).

#### **3.1            Data Synthesis**

The 3-D simulation model of North [1989] will be extended to consider a specific imaging system: differentially polarized 4-lens 35-mm panchromatic photography; the photographs are digitally scanned to produce TIFF (or similar format) digital images; the digital images are combined to form the Stokes' parameter images; and these images are transformed into their spatial spectra via the forward 2-D Fast Fourier Transform (FFT). This model will attempt to simulate the actual imaging process that will be executed during the Data Collection and Data Analysis phases.

A parametric exploration of the model will then be exercised in order to predict the polarized imaging conditions that optimize spatial information content. The primary figure-of-merit for making this determination is the amount of correlation between the actual (modeled) waterwave slope spectra and their reconstruction from the polarized radiance image spectra. Other beneficial figures-of-merit



may be considered during this phase of research.

One secondary objective (resources permitting) is to compare the results of this model with another simulation model, e.g., SENSAT, using the same input parameters. A correlation of results between the two models would provide an added measure of confidence in the model predictions that will be carried into the later research phases.

### 3.2 Data Collection

Differentially polarized 4-lens 35-mm panchromatic photography of various natural water surfaces will be collected in the field under natural illumination conditions. Imaging geometries, number of redundant images, and requirements for control and baseline images will be determined from the predictions of the Data Synthesis phase, above.

A Nishika, Nimslo, or similar 4-lens camera will be modified to produce the polarized images. One option is to mount a polarizing filter over each of the four lenses, each filter rotated at a different angle about the optical axis, e.g.,  $0^\circ$ ,  $45^\circ$ ,  $90^\circ$ , and  $135^\circ$ . Another option is to mount only three polarizing filters over three lenses, e.g.,  $0^\circ$ ,  $60^\circ$ , and  $120^\circ$ , and use the fourth lens to create an unpolarized calibration image.

The key advantage of using a single-body 4-lens camera is that the synoptic polarized images are exposed on the same roll of film: the sensitometry is equivalent for all the four-image sets on each film roll. However, a calibration step wedge will be imaged on each roll of film in order to establish a Density-versus-log(Exposure) curve for within-roll and between-roll calibration. This exposure calibration is important to the accurate measurement of signal-to-noise and contrast which, in turn, are key inputs to feature recognition and reconstruction algorithms (e.g., surface slope spectrum reconstruction).

The photographs will be digitized by an image scanner. One option is to commercially digitize the photos onto compact disks, e.g., via the Kodak Photo CD™ process. A second option is to procure a 35-mm slide scanner, e.g., the Nikon Coolscan™ LED scanner, and digitize the images for direct transfer onto computer memory, hard disk, or other media. These digital images will be maintained as TIFF, or similar format, data files. The advantage of the second option over the first option is direct calibration control of the digitalization process, to include the selection of the scanning resolution.

One option for investigation is to apply an additional narrowband spectral filter over the lenses. Restriction to red-bandpass imaging, for example, should reduce the upwelling subsurface radiance component in the image; blue-bandpass imaging,

on the other hand, should enhance it.

One secondary objective (resources permitting) is to collect polarized photography of waterwave scenes containing Secchi disks suspended at various water depths under varying conditions of turbidity. This secondary investigation would provide useful calibration data on the upwelling subsurface radiance that is present in the polarized imagery; as an independent water penetration study, it could demonstrate the utility of polarized imagery, compared with unpolarized imagery, in the detection of subsurface features through the differential reduction of unwanted polarized reflected surface radiance.

Another secondary objective (resources permitting) is to collect polarized photography of shadowed areas (high solar and/or high sensor zenith angle) containing a shadowed target. This independent investigation could demonstrate the utility of polarized imagery, compared with unpolarized imagery, in the detection of shadowed features through the differential selection of polarized sky radiance reflecting from the shadows.

### 3.3 Data Analysis

The synoptic TIFF images are digitally combined to form the Stokes' parameter images. These images are then transformed into their spatial spectra via the forward 2-D Fast Fourier Transform

(FFT). If required, multiple sequential realizations of the spectra may be combined to provide statistical stability. One option for investigation would first FFT the uncombined TIFF images and then evaluate combinations (sum, difference, ratio) of their 2D spectra.

The majority of the analysis is expected to involve the evaluation of those polarized image spectra that demonstrate significant deviations in their distribution of spectral energy relative to the unpolarized image spectra for the same imaging conditions: measure their ranges of spatial frequency and imaging azimuth, measure their spectral contribution to the total variance of the scene.

The polarized spectra of the measured imagery will be compared with their equivalent synthetic spectra to determine the degree of correlation between the synthetic and measured imagery. It is anticipated that substantial analysis may be devoted to a normalization or reconciliation between the two sets of results. The outcome of a reconciliation may require modification of the simulation model, re-calibration of the imaging system, and / or discussion of any irreconcilable differences and their possible sources.

The expected study results are the correlation sensitivity analysis of the simulation model data, reconciliation with the actual image data, a comparison of analytic methods, an

identification of methods that provide optimum results, any unexpected results, a recapitulation of the study objectives, and finally, suggestions for further research.

**4.0****SCHEDULE**

<b>MILESTONE</b>	<b>NOT EARLIER THAN</b>	<b>NOT LATER THAN</b>
<b>Submit Proposal</b>	<b>Spring Start 94</b>	<b>Spring End 94</b>
<b>Complete Model</b>	<b>Summer Start 94</b>	<b>Summer End 94</b>
<b>Analyze Model</b>	<b>Summer Start 94</b>	<b>Summer End</b>
<b>Collect Data</b>	<b>Mid-Summer 94</b>	<b>Mid-Fall 94</b>
<b>Analyze Data</b>	<b>Mid-Fall 94</b>	<b>Mid-Spring 95</b>
<b>Complete Thesis</b>	<b>Mid-Spring 95</b>	<b>Mid-Summer 95</b>
<b>Defend Thesis</b>	<b>Spring End 95</b>	<b>Summer End 95</b>

## 5.0

## REFERENCES

- Abshire, J.B. & J.F. McGarry, "Two-color short-pulse laser altimeter measurements of ocean surface backscatter", in *Applied Optics*, 26(7), pp 1304-1310, 1987.
- Barber, N.F., "A diffraction analysis of a photograph of the sea", in *Nature*, 164(4168), pp 485, 1949.
- Barber, N.F., "Finding the direction of travel of sea waves", in *Nature*, 174(4440), pp 1048-1050, 1954.
- Beckmann, P. & A. Spizzichino, The Scattering of Electromagnetic Waves from Rough Surfaces, Macmillan Company, New York, 1963.
- Carlson, G.E., "Estimation of ocean wave wavenumber and propagation direction from limited synthetic aperture radar data", in *IEEE Transactions on Geoscience and Remote Sensing*, GE-22(6), pp 609-614, 1984.
- Cartwright, D.E. & M.S. Longuet-Higgins, "The statistical distribution of the maxima of a random function", in *Proceedings of the Royal Society*, A237(1209), pp 212-232, 1956.
- Chapman, R.D. & G.B. Irani, "Errors in estimating slope spectra from wave images", in *Applied Optics*, 20(20), pp 3645-3652, 1981.
- Cote, L.J., J.O Davies, W. Marks, R.J. McCough, E. Mehr, W.J. Pierson, J.F. Ropek, G. Stephenson & R.C. Vetter, "The directional spectrum of a wind-generated sea as determined from data obtained by the stereo wave observation project", in *Meteorological Papers*, NYU College of Engineering, 2(6), 1960.
- Coulson, K.L., Solar and Terrestrial Radiation, Academic Press, New York, 1975.
- Cox, C.S. & W.H. Munk, "Measurement of the roughness of the sea surface from photographs of the sun's glitter", in *Journal of the Optical Society of America*, 44(11), pp 838-850, 1954a.
- Cox, C.S. & W.H. Munk, "Statistics of the sea surface derived from sun glitter", in *Journal of Marine Research*, 13(2), pp 198-227, 1954b.
- Duggin, M.J., S.A. Israel, V.S. Whitehead, J.S. Myers & D.R. Robertson, "Use of polarization methods in earth resources investigations", in *Proceedings of the SPIE*, 1166, pp 11-22, 1989.

Fisher, M.G., Oceanographic Analysis of Sun Glint Images Taken on Space Shuttle Mission STS 41-G, M.S. Thesis, Naval Postgraduate School, 1986.

Gotwols, B.L. & G.B. Irani, "Optical determination of the phase velocity of short gravity waves", in Journal of Geophysical Research, 85(C7), pp 3964-3970, 1980.

Gotwols, B.L. & G.B. Irani, "Charge-coupled device camera system for remotely measuring the dynamics of ocean waves", in Applied Optics, 21(5), pp 851-860, 1982.

Hasselmann, D.E., M. Dunckel & J.A. Ewing, "Directional wave spectra observed during JONSWAP 1973", in Journal of Physical Oceanography, 10, pp 1264-1280, 1980.

Holthuijsen, L.H., "Observations of the directional distribution of ocean-wave energy in fetch limited conditions", in Journal of Physical Oceanography, 13(2), pp 191-207, 1983a.

Holthuijsen, L.H., "Stereophotography of ocean waves", in Applied Ocean Research, 5(4), pp 204-209, 1983b.

Hulburt, E.O., "The polarization of light at sea", in Journal of the Optical Society of America, 24, pp 35-42, 1934.

Israel, S.A., Analysis of Space Shuttle and Video Polarization Imagery, M.S. Thesis, SUNY CESP, Syracuse NY, 1991.

Kasevich, R.S., C.H. Tang & S.W. Henriksen, "Energy spectra of sea waves for photographic interpretation", in Proceedings of the Seventh International Symposium on Remote Sensing of the Environment, pp 607-624, University of Michigan, Ann Arbor, 1971.

Kasevich, R.S., C.H. Tang & S.W. Henriksen, "Analysis and optical processing of sea photographs for energy spectra", in IEEE Transactions on Geoscience and Electronics, GE-10(1), pp 51-58, 1972.

Kasevich, R.S., "Directional wave spectra from daylight scattering", in Journal of Geophysical Research, 80(33), pp 4535-4541, 1975.

Keller, W.C. & B.L. Gotwols, "Two-dimensional optical measurement of wave slope", in Applied Optics, 22(22), pp 3476-3478, 1983.

Kinsman, B., Wind Waves: their generation and propagation on the ocean surface, Prentice Hall, Englewood Cliffs NJ, 1965.

Konnen, G.P., Polarized light in Nature, Cambridge University Press, Cambridge England, 1985.



- Longuet-Higgins, M.S., "On the statistical distribution of the heights of sea waves", in *Journal of Marine Research*, 11(3), pp 245-266, 1952.
- Longuet-Higgins, M.S., "Statistical properties of a moving waveform", in *Proceedings of the Cambridge Philosophical Society*, 52(2), pp 234-245, 1956.
- Longuet-Higgins, M.S., "The statistical analysis of a random moving surface", in *Philosophical Transactions of the Royal Society*, A249(966), pp 321-387, 1957.
- Longuet-Higgins, M.S., "On the interval between successive zeros of a random function", in *Proceedings of the Royal Society*, A246, pp 99-118, 1958.
- Longuet-Higgins, M.S., "Reflection and refraction at a random moving specular point", Parts I, II & III in *Journal of the Optical Society of America*, 50(9), pp 838-856, 1960.
- Longuet-Higgins, M.S., "The directional spectrum of ocean waves, and processes of wave generation", in *Proceedings of the Royal Society*, A265(1322), pp 286-315, 1962.
- Lybanon, M., "Ocean wave slope statistics from automated analysis of sun glitter photographs", *NORDA Report 103*, 1985.
- Marks, W., "The use of a filter to sort out directions in a short-crested sea surface", in *Transactions of the American Geophysical Union*, 35(5), pp 758-766, 1954.
- Marks, W. & F.C. Ronne, "Aerial stereo-photography and ocean waves", in *Photogrammetric Engineering & Remote Sensing*, 21, pp 107-110, 1955.
- Maul, G.A., Introduction to Satellite Oceanography, Martinus Nijhoff Publishers, Dordrecht Netherlands, 1985.
- McLeish, W., "Spatial spectra of ocean surface temperature", in *Journal of Geophysical Research*, 75(33), pp 6872-6877, 1970.
- Monaldo, F.M. & R.S. Kasevich, "Optical determination of short-wave modulation by long ocean gravity waves", in *IEEE Transactions on Geoscience and Remote Sensing*, GE-20(3), pp 254-259, 1982.
- Monaldo, F.M. & D.R. Lyzenga, "On the estimation of wave slope- and height-variance spectra from SAR imagery", in *IEEE Transactions on Geoscience and Remote Sensing*, GE-24(4), pp 543-551, 1986.
- North, J.A., Fourier Image Synthesis and Slope Spectrum Analysis

- of Deepwater, Wind-wave Scenes Viewed at Brewster's Angle, M.S. Thesis, Rochester Institute of Technology NY, 1989.
- Palm, C.S., R.C. Anderson & A.M. Reece, "Laser probe for measuring 2-D wave slope spectra of ocean wave capillary waves", in *Applied Optics*, 16(4), pp 1074-1081, 1977.
- Pierson, W.J., Jr. & W. Marks, "The power spectrum analysis of ocean wave records", in *Transactions of the American Geophysical Union*, 33(6), pp 834-844, 1952.
- Pierson, W.J., Jr. & R.A. Stacy, "The elevation, slope, and curvature spectra of a wind roughened sea surface", NASA Contractor Report 2247, 1973.
- Plass, G.N., Kattawar & J.A. Guinn, Jr., "Radiative transfer in the earth's atmosphere and ocean: influence of ocean waves", in *Applied Optics*, 14(8), pp 1924-1936, 1975.
- Plass, G.N., Kattawar & J.A. Guinn, Jr., "Radiance distribution over a ruffled sea: contributions from glitter, sky, and ocean", in *Applied Optics*, 15(12), pp 3161-3165, 1976.
- Pos, J.D., L.P. Adams & F.A. Kilner, "Synoptic wave height and pattern measurements in laboratory wave basins using close-range photogrammetry", in *Photogrammetric Engineering and Remote Sensing*, 54(12), pp 1749-1756, 1988.
- Powell, W.M., & G.L. Clarke, "The reflection and absorption of daylight at the surface of the sea", in *Journal of the Optical Society of America*, 26, pp 111-120, 1936.
- Prosch, T., D. Hennings & E. Raschke, "Video polarimetry: a new technique in atmospheric science", in *Applied Optics*, 22(9), pp 1360-1363, 1983.
- Robinson, I.S., Satellite Oceanography, an introduction for oceanographers and remote-sensing scientists, Ellis Horwood Limited, West Sussex England, 1985.
- Saunders, P.M., "Shadowing on the ocean and the existence of the horizon", in *Journal of Geophysical Research*, 72(18), pp 4643-4649, 1967.
- Saunders, P.M., "Radiance of sea and sky in the infrared window 800-1200  $\text{cm}^{-1}$ ", in *Journal of the Optical Society of America*, 58(5), pp 645-652, 1968.
- Sawyer, D.W., "Preliminary report on the determination of water surface profiles", U.S. Naval Photographic Interpretation Center Report 103-49, 1949.

- Schau, H.C., "Measurement of capillary wave slopes on the ocean" in *Applied Optics*, 17(1), pp 15-17, 1978.
- Schooley, A.H., "A simple method for measuring the statistical distribution of water wave surfaces", in *Journal of the Optical Society of America*, 44(1), pp 37-40, 1954.
- Schwartz I.B. & D. Hon, "Emissivity as a function of surface roughness: a computer model", NRL Report (unpublished).
- Sheres, D., Remote Synoptic Surface Flow Measurements in Small Bodies of Water, Ph.D. Dissertation, University of California, San Diego, 1980.
- Sheres, D., "Remote and synoptic water-wave measurements by aerial photography: a model, experimental results, and an application", in *IEEE Journal of Oceanic Engineering*, OE-6(2), pp 63-69, 1981.
- Sidran, M., "Broadband reflectance and emissivity of specular and rough water surfaces", in *Applied Optics*, 20(18), pp 3176-3183, 1981.
- Spitzer, D. & D. Arief, "Relationship between the sky radiance reflected at the sea surface and the downwelling irradiance", in *Applied Optics*, 22(3), pp 378-379, 1983.
- Stewart, R.H., Methods of Satellite Oceanography, University of California Press, Berkeley & Los Angeles CA, 1985.
- Stilwell, D., Jr., "Directional energy spectra of the sea from photographs", in *Journal of Geophysical Research*, 74(8), pp 1974-1986, 1969.
- Stilwell, D., Jr. & R.O. Pilon, "Directional spectra of surface waves from photographs", in *Journal of Geophysical Research*, 79(9), pp 1277-1284, 1974.
- Weinman, J.A., "Derivation of atmospheric extinction profiles and wind speed over the ocean from a satellite-borne lidar", in *Applied Optics*, 27(19), pp 3994-4001, 1988.
- Wu, J., "Slope and curvature distributions of wind-disturbed water surfaces", in *Journal of the Optical Society of America*, 61(7), pp 852-858, 1971.